

Neuronal Oscillations and Functional Interactions Between Resting State Networks: Effects of Alcohol Intoxication

Xu Lei,^{1*} Yulin Wang,¹ Hong Yuan,¹ and Dante Mantini^{2,3}

¹Key Laboratory of Cognition and Personality (Ministry of Education) and School of Psychology, Southwest University, Chongqing, China

²Department of Experimental Psychology, University of Oxford, Oxford, United Kingdom

³Department of Health Sciences and Technology, ETH Zurich, Zurich, Switzerland



Abstract: Functional magnetic imaging (fMRI) studies showed that resting state activity in the healthy brain is organized into multiple large-scale networks encompassing distant regions. A key finding of resting state fMRI studies is the anti-correlation typically observed between the dorsal attention network (DAN) and the default mode network (DMN), which—during task performance—are activated and deactivated, respectively. Previous studies have suggested that alcohol administration modulates the balance of activation/deactivation in brain networks, as well as it induces significant changes in oscillatory activity measured by electroencephalography (EEG). However, our knowledge of alcohol-induced changes in band-limited EEG power and their potential link with the functional interactions between DAN and DMN is still very limited. Here we address this issue, examining the neuronal effects of alcohol administration during resting state by using simultaneous EEG-fMRI. Our findings show increased EEG power in the theta frequency band (4–8 Hz) after administration of alcohol compared to placebo, which was prominent over the frontal cortex. More interestingly, increased frontal tonic EEG activity in this band was associated with greater anti-correlation between the DAN and the frontal component of the DMN. Furthermore, EEG theta power and DAN-DMN anti-correlation were relatively greater in subjects who reported a feeling of euphoria after alcohol administration, which may result from a diminished inhibition exerted by the prefrontal cortex. Overall, our findings suggest that slow brain rhythms are responsible for dynamic functional interactions between brain networks. They also confirm the applicability and potential usefulness of EEG-fMRI for central nervous system drug research. *Hum Brain Mapp* 35:3517–3528, 2014. © 2013 Wiley Periodicals, Inc.

Key words: functional connectivity; alcohol; anti-correlated networks; simultaneous EEG-fMRI



Contract grant sponsor: National Nature Science Foundation of China; Contract grant number: 31200857; Contract grant sponsor: National Key Discipline of Basic Psychology at Southwest University; Contract grant number: NSKD11047; Contract grant sponsor: Humanity and Social Science Youth foundation of Ministry of Education of China; Contract grant number: 12YJC190015; Contract grant sponsor: Swiss National Science Foundation; Contract grant number: 320030_146531; Contract grant sponsor: Seventh Framework Programme of the European Commission; Contract grant number: PCIG12-334039

*Correspondence to: Xu Lei, School of Psychology, Southwest University, Chongqing 400715, China. E-mail: xlei@swu.edu.cn

Received for publication 5 June 2013; Revised 15 August 2013; Accepted 27 September 2013.

DOI 10.1002/hbm.22418

Published online 25 November 2013 in Wiley Online Library (wileyonlinelibrary.com).

INTRODUCTION

The study of interactions between distant brain regions is becoming increasingly important, since perception, cognition, and behavior are not just the result of neuronal computations in isolated brain regions but require the exchange of information between highly specialized but distributed neuronal assemblies [Bressler and Menon, 2010]. Functional magnetic resonance imaging (fMRI) studies in individuals at rest have revealed that the brain has a hierarchical organization [Lee et al., 2012], and on a large scale consists of two broad systems that operate in apparent competition or antagonism with each other [Fox et al., 2005; Fransson, 2006]. These two systems largely overlap with the default mode network (DMN), which is thought to support internally oriented processing [Buckner et al., 2008; Lei et al., 2013; Mantini and Vanduffel, 2013], and the dorsal attention network (DAN), which primarily mediates goal-directed attention processes [Corbetta and Shulman, 2002; Fornito et al., 2012]. Individuals with stronger DMN-DAN anti-correlation displayed shorter and less variable reaction times during performance of cognitive control tasks [De Pisapia et al., 2012; Kelly et al., 2008]. Thus, an emerging concept is that increased anti-correlation between these two brain networks is an index of efficient cognitive processing [De Pisapia et al., 2012; Kelly et al., 2008].

To explore the electrophysiological correlates of brain network activity, several studies have combined fMRI with concurrent electroencephalography (EEG) to examine how neuronal oscillations in different frequency bands, the so-called brain rhythms, contribute to large-scale brain networks [Ganzetti and Mantini, 2013; Laufs et al., 2003; Mantini et al., 2007b]. However, the relationship between neuronal oscillations and brain network interactions is still poorly understood. EEG and fMRI studies have documented that both brain rhythms and network interactions can be experimentally modulated by administration of small amount of alcohol at rest. Specifically, EEG studies showed that alcohol administration induced an increase in the power of the theta rhythm [Schwarz et al., 1981], mainly located over the frontal cortex [Tran et al., 2004] and persistent up to two hours after ingestion [Ehlers et al., 1989]. fMRI investigations revealed changes in cortical activation after alcohol intoxication [Calhoun et al., 2004; Levin et al., 1998]. Dose-dependent increases were identified in insula, dorsolateral prefrontal cortex, and precentral regions, which belong to the DAN; dose-dependent decreases were observed in middle frontal areas, anterior and posterior cingulate, precuneus, which are core areas of the DMN [Calhoun et al., 2004].

On the basis of the EEG and fMRI findings mentioned above, we hypothesized that the anti-correlation between DMN and DAN may be increased after alcohol administration, and that this change may be related to changes in neuronal oscillations, particularly in the theta frequency band. To test this hypothesis, we conducted a simultane-

ous EEG-fMRI study in healthy subjects at rest, who were administered a moderate dose of either alcohol or placebo. This resting-state experiment allowed us to gain new insights into how specific neuronal oscillations sustain functional interactions between large-scale networks.

MATERIALS AND METHODS

Participants

Fifteen healthy subjects (seven females) participated in both alcohol and placebo sessions in a counter-balanced manner. All participants, recruited from the local community through advertisements, ranged between 21 and 24 years (mean = 22.2, SD = 1.2) of age. They were without any history of psychiatric or neurological illness as confirmed by psychiatric clinical assessment. All had normal or corrected-to-normal vision, and free from any neurological or psychiatric disorder. All recruited subjects consumed alcohol less than two times a month and fewer than 100 mL at a time, and were therefore classified as light or moderate drinkers. Participants who met criteria for alcohol abuse or dependence, or who had never drunk alcohol were excluded from the experiment. Participants were instructed to refrain from smoking and from consuming any food or drink containing alcohol and/or caffeine for 24 h before scanning, and to eat a light meal (avoiding fatty food) on the morning of the scanning day. Written informed consent was obtained after detailed explanation of the study protocol, which was approved by the Ethics Committee of Southwest University. All procedures were conducted in accordance with the sixth revision of the Declaration of Helsinki.

Experiment Design and Euphoria Rating

Drinks were made with orange or kiwifruit juice to constant volume of 350 mL. For the alcohol session only, alcohol was added according to an individually tailored dose of 0.7 ml/kg. This quantity was calculated based on weight to reach a moderate blood alcohol concentration (BAC). BAC was measured using a hand-held breathalyzer calibrated using an ethanol breath standard sample dispensing device.

The alcohol and placebo recording sessions were carried out on two separate days. In the alcohol session, a simultaneous EEG-fMRI recording was taken 60 min after alcohol administration. In the placebo session, an identical recording was taken exactly at the same time of day to avoid confounds from circadian variability. The participant was instructed to simply lie inside the scanner with eyes closed. She/he was also asked to remain awake during the experiment. No visual or auditory stimuli were presented at any time during the functional scanning.

After each EEG-fMRI recording session, the participant rated the change in the level of euphoria compared to his/

her condition before drinking (−2: largely decreased euphoria; −1: moderately decreased euphoria; 0: no change; 1: moderately increased euphoria; 2: largely increased euphoria). Subsequently, she/he was brought to a room where she/he watched movies, surfed the internet, rested or slept. Food and water were also provided. A medical doctor determined when it was safe for the participant to leave and discharged her/him.

Simultaneous EEG/fMRI Recording

The EEG was digitized at 5 kHz, referenced online to FCz using a nonmagnetic MRI-compatible EEG system (BrainAmp MR plus, Brain products, Munich, Germany). All 32 electrodes were ring-type sintered nonmagnetic Ag/AgCl electrodes, placed on the scalp according to the international 10/20 system. An additional electrode was dedicated to the electrocardiogram (ECG). The EEG amplifier, along with a rechargeable power pack was placed about 15 cm outside the bore. The amplified and digitized EEG signal was transmitted via fiber optic cables to the recording computer placed outside the scanner room.

A high-resolution T1-weighted structural volume was acquired using a 3T Siemens Trio scanner. The 3D spoiled gradient recalled (SPGR) sequence used the following parameters: TR/TE = 8.5/3.4 ms, FOV = 240 × 240 mm², flip angle = 12°, acquisition matrix = 512 × 512, thickness = 1 mm with no gap. The high-resolution T1-weighted structural volume provided an anatomical reference for the functional scan. Subsequently, fMRI scanned 200 functional volumes, using an EPI sequence with the following parameters: TR/TE = 1,500/29 ms, FOV = 192 × 192 mm², flip angle = 90°, acquisition matrix = 64 × 64, thickness/gap = 5/0.5 mm, in-plane resolution = 3.0 × 3.0 mm², axial slices = 25. The first six volumes were discarded to ensure steady-state longitudinal magnetization. Head movements were minimized by using a cushioned head fixation device.

EEG Data Processing

EEG data was preprocessed to remove gradient and ballistocardiographic (BCG) artifacts. The FMRIB toolbox in EEGLAB (www.sccn.ucsd.edu/eeglab) was used for off-line correction of the MRI imaging artifact [Niazy et al., 2005]. This software implements the adaptive artifact subtraction (AAS) method, in which the MRI imaging artifact waveforms are segmented, averaged and iteratively subtracted from the EEG signals [Allen et al., 2000]. Subsequently, data were down-sampled to 250 Hz and digitally filtered within the 1 to 30 Hz frequency band using a Chebyshev II-type filter with 40 dB attenuation and zero-phase distortion. We further examined the EEG signals, and we removed data segments clearly contaminated by muscle activity. Accordingly, only 190 to 275 s (225 ± 32 s) of continuous EEG recordings were remained. The EEG data were processed using temporal independent compo-

nent analysis (ICA) to attenuate BCG artifact, the ocular and the residual imaging artifact [Mantini et al., 2007a].

The filtered EEG recordings were re-referenced to average reference for further analyses. A digital FFT-based power spectrum analysis (Welch technique, Hanning windowing function, no phase shift) computed power density of the EEG rhythms. The following standard band frequencies were studied: delta (2–4 Hz), theta (4–8 Hz), alpha 1 (8–10.5 Hz), alpha 2 (10.5–13 Hz), beta 1 (13–20 Hz), and beta 2 (20–30 Hz). These band frequencies were selected on the basis of previous relevant EEG studies [Lukas et al., 1986; Sanz-Martin et al., 2011]. In order to approximate a normal distribution, the power value was transformed into logarithms ($10 \times \log_{10} (\mu V^2/Hz)$) before statistical analysis.

fMRI Data Processing

The resting state fMRI data were preprocessed using SPM8 (<http://www.fil.ion.ucl.ac.uk/spm/>), developed by the Wellcome Department of Cognitive Neurology, London, UK. The preprocessing steps included slice timing, head motion correction, spatial normalization, smoothing, and linear trend removal. Two subjects were excluded due to excessive (>1 mm) head motion during scanning, leaving us with 13 subjects for our analyses.

After fMRI data preprocessing, we performed spatial ICA using GIFT (<http://icatb.sourceforge.net/>) [Calhoun et al., 2001a] to retrieve resting state networks and subsequently identify our networks of interest. The optimal number of components was set to 20, which was estimated using the minimum description length criterion [Li et al., 2007]. Previous fMRI studies using ICA suggested that 20 independent components can provide a reliable representation of large-scale networks [Calhoun et al., 2001b; Zuo et al., 2010]. After data reduction by principal component analysis (PCA), we performed ICA decomposition on concatenated datasets using the Extended Infomax algorithm. Independent components (ICs) and time courses were back-reconstructed for each subject, and the mean spatial maps for each group were transformed to z-scores for display purposes. We employed the DAN and DMN maps from one of our previous resting state fMRI studies [Mantini et al., 2013] as spatial templates for component classification. The selected networks corresponded to those components with the largest spatial correlations with the templates [Chang et al., 2013; Mantini et al., 2009] and with correlation values at least double that of all other networks. We visually inspected all ICs to confirm that the automated IC selection worked correctly [Zuo et al., 2010]. The time-courses of the selected components were used as input for correlation analyses.

Network interactions during alcohol and placebo sessions were assessed by computing pair-wise correlations between the time-courses of DMN and DAN components. Before computing correlations between time-courses, we

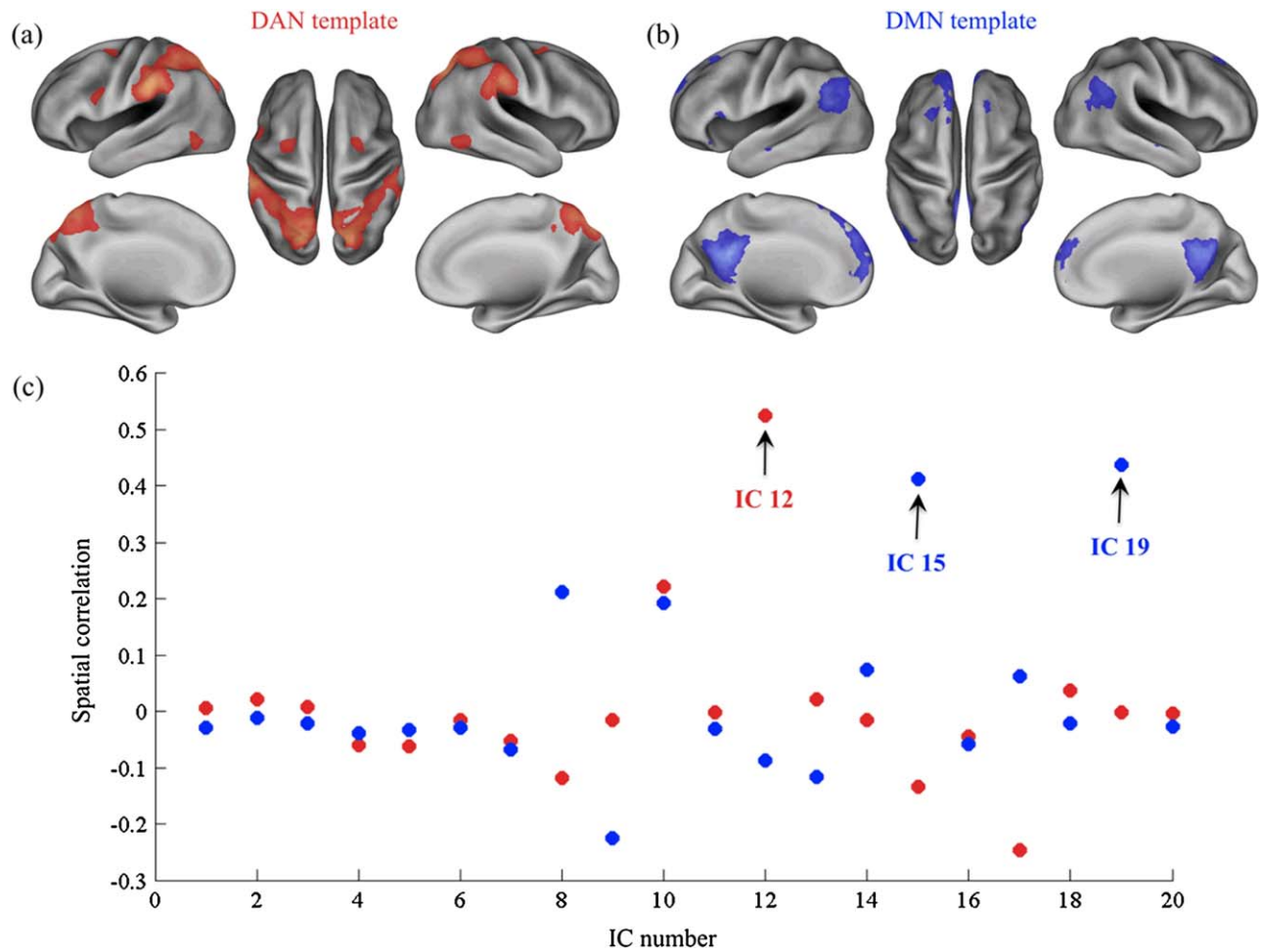


Figure 1.

Selection of independent components (ICs) using DAN and DMN templates. The DAN (a) and DMN (b) templates are colored red and blue respectively, and are overlaid onto a standard cortical model (left and right lateral, left and right medial, and dorsal views). (c) The scatter plot shows the spatial correlations

between each IC map and the templates maps (red dots for DAN, blue dots for DMN). The selected ICs are indicated with a black arrow. [Color figure can be viewed in the online issue, which is available at wileyonlinelibrary.com.]

removed the effects of spurious signal variations, including head-movement parameters and average signals arising from the ventricles, white matter and whole brain (the so-called global signal), by means of linear regression [Van Dijk et al., 2010]. As the use of the global signal is a controversial issue [Fox et al., 2009], we also repeated our analysis without global signal regression and tested if the results remained. The correlation values were transformed to *z*-values using the Fisher's *r*-to-*z* transform before further statistical analyses.

Statistical Analysis

The paired *t*-test was used for euphoria rating to identify significant changes between alcohol and placebo

sessions. A statistical analysis was conducted for EEG power values and fMRI network interactions in different subjects using a two-factor analysis of variance (ANOVA). One within-subject factor is beverage (alcohol and placebo), and another is frequency band (EEG) or network pair (fMRI). We also employed post hoc paired *t*-tests to further identify significant changes between alcohol and placebo sessions. The differences were considered significant if the associated probability was below 0.05, after correction for multiple comparisons using the Bonferroni method. We used the Spearman correlation to assess the correspondence between fMRI network interactions and grand averaged EEG power across subjects. We also calculated Spearman correlations between fMRI network interactions and single-channel

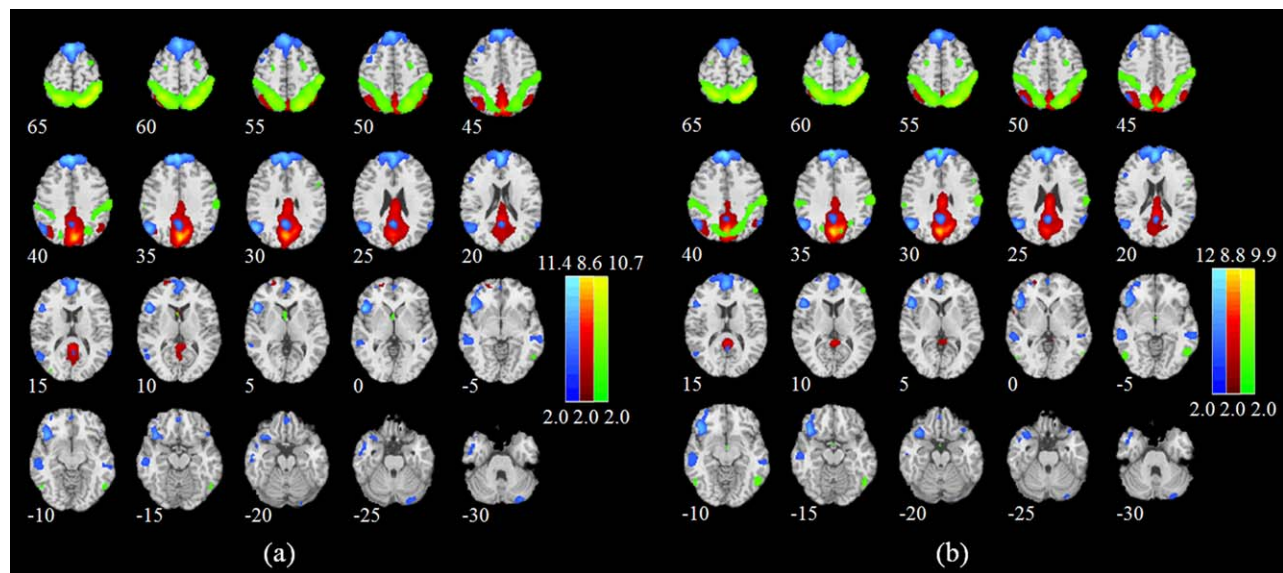


Figure 2.

Group-level maps for the anterior and posterior DMN (aDMN and pDMN, respectively) and the DAN in (a) placebo and (b) alcohol sessions. Brain areas with intensities of two standard deviations greater than the mean are shown. The aDMN, pDMN, and DAN are colored in blue, red, and green, respectively. [Color figure can be viewed in the online issue, which is available at wileyonlinelibrary.com.]

EEG power to identify the spatial distribution of EEG-fMRI coupling.

RESULTS

Self-Reports of Alcohol Effects

All subjects drank full doses of either alcohol or placebo without feeling discomfort. In the placebo administration session, the BAC was 0.00 mg/dl for all subjects and the level of euphoria remained unchanged. In the alcohol administration session, the BAC was 57.08 ± 6.41 mg/dl just before the scan. The subjective rating of ethanol-induced euphoria was significantly increased ($t = 3.950$, $P = 0.0019$) compared to the placebo session. Four subjects reported a feeling of greatly heightened euphoria after administration of alcohol, and were also more talkative than before the session. Six subjects experienced a moderate increase of euphoria, whereas two subjects reported no difference and one subject reported diminished ethanol-induced euphoria after alcohol consumption.

Increased DMN-DAN Anticorrelation

By applying spatial ICA to resting-state fMRI data, we identified the dorsal attention network (DAN), as well as two networks corresponding to the DMN. These were selected from among the 20 components retrieved by ICA

using independent DAN and DMN templates obtained from a previous study [Mantini et al., 2013]. Specifically, we selected the independent components using a spatial map largely overlapping with the network template, as measured by spatial correlation (Fig. 1). This selection was then confirmed by careful visual inspection of the IC maps.

Overall, the spatial distribution of the three selected networks was for the most part similar between alcohol and placebo sessions (Fig. 2). The first network, which corresponded to the DAN, included the right part of the inferior precentral sulcus and two bilateral pairs of frontal eye fields, and the middle temporal motion complex. The second network corresponded to the anterior portion of the DMN (aDMN), and encompassed medial prefrontal cortex, posterior cingulate/retrosplenial cortex and bilateral inferior frontal gyrus. The third network overlapped more closely with the posterior part of the DMN (pDMN) and encompassed precuneus, posterior cingulate cortex, and bilateral angular cortex (Fig. 2 and Table I).

We also examined the functional interactions between the three networks. On a general level, we found positive correlations between aDMN and pDMN, whereas the correlation between these two networks and the DAN was negative (Figs. 3 and 4). We conducted a two-factor ANOVA on these correlations, testing for main effects and interaction of beverage (alcohol and placebo) \times network pair (aDMN-DAN and pDMN-DAN). This analysis showed a main effect of beverage ($F_{(1,12)} = 7.04$, $P = 0.0108$). No significant

TABLE I. Peak foci for the group-level DAN, aDMN and pDMN defined by ICA on alcohol and placebo sessions together

Regions	MNI coordinates			No. voxels
aDMN				
Medial prefrontal cortex	-1	58	9	518
Posterior cingulate/ retrosplenial cortex	-3	49	29	66
Dorsal medial prefrontal cortex	-8	50	34	360
L Anterior temporal lobe	-55	-10	-20	34
L Inferior frontal gyrus	-43	26	-8	267
R Inferior frontal gyrus	45	32	-13	189
L lateral parietal cortex	-53	-67	27	62
R lateral parietal cortex	56	-65	32	22
pDMN				
Posterior cingulate cortex	-2	-48	28	248
L Posterior inferior parietal lobule	-49	-60	33	132
Precuneus	1	-60	42	1023
L Angular	-54	-63	33	470
R Angular	45	-63	48	151
DAN				
R Inferior precentral sulcus	51	8	33	57
R Ventral inferior parietal sulcus	38	-80	23	32
L Frontal eye fields	-24	-2	56	11
R Frontal eye fields	24	-2	56	14
L Middle temporal motion complex	-51	-66	-7	62
R Middle temporal motion complex	54	-54	-6	63
L Superior occipital gyrus	-18	-66	59	43
R Superior occipital gyrus	26	-56	60	68
L Superior parietal lobule	-31	-48	52	400
R Superior parietal lobule	38	-46	54	572
L Inferior parietal sulcus	-25	-69	51	558
R Inferior parietal sulcus	23	-60	58	215

The significance threshold was set to $P < 0.01$ FDR-corrected, with a minimum cluster size equal to 10 adjacent voxels.

DAN, dorsal attention network; aDMN, anterior default mode network; pDMN, posterior DMN; L, left hemisphere; R, right hemisphere.

effect of network pair ($F_{(1,12)} = 3.6$, $P = 0.0637$), or interaction between beverage and network pair ($F_{(1,12)} = 0.4$, $P = 0.5286$), was found. Paired t -tests between correlations in the alcohol and placebo sessions indicated a significant increase, from -0.21 to -0.44 , in anticorrelation between the DAN and aDMN ($P = 0.0043$). Similarly, we found an increase in anticorrelation between DAN and pDMN, from -0.12 to -0.26 , which was however not significant ($P = 0.0737$). Finally, an analysis of correlation without global signal regression revealed the same effects.

The EEG Signature of the Anticorrelation

We analyzed the absolute power spectrum of the EEG recordings across subjects, thereby assessing which band

the main spectral changes induced by alcohol intoxication occur in. By directly comparing the results for the alcohol and placebo sessions, we observed a clear increase in the power of the theta rhythm (Fig. 5). Thus, we sought to test the hypothesis that this increased theta power in the alcohol session is accompanied by an increased DMN-DAN anti-correlation. Consistent with this hypothesis, we found a significant relationship ($r = -0.7692$, $P = 0.0033$) between the aDMN-DAN anticorrelation and the grand-average EEG theta power across subjects (Fig. 6). However, we did not find a similar relationship between the pDMN-DAN anti-correlation and the grand-average EEG theta power ($r = -0.0055$, $P = 0.9928$). Furthermore, it is likely that this effect can be ascribed to the prefrontal theta rhythm, as suggested by a parallel analysis conducted for each EEG recording rather than using grand-average EEG activity (Fig. 6).

Neither the correlation between the euphoria ratings and changes in DMN-DAN interaction, nor the correlation between the euphoria ratings and theta power were significant. However, they were both close to significance ($P = 0.0517$ and $P = 0.0721$, respectively). Interestingly, the four subjects who reported feeling intense euphoria after alcohol consumption had the largest overall changes in aDMN-DAN interaction and theta EEG power (see pink diamonds outlined in black in the top-left panel of Fig. 6).

The specificity of this effect in the theta band was demonstrated by replicating the same analysis for different frequency bands (Fig. 7). Before that, we conducted a two-factor ANOVA on absolute power of EEG, testing for main effects and interaction of beverage (alcohol and placebo) \times frequency band (delta, theta, alpha 1, alpha 2, beta 1, and beta 2). The ANOVA results showed a significant main effect of frequency band ($F_{(5,13)} = 30.62$, $P < 0.001$), but not of beverage ($F_{(1,13)} = 0.44$, $P = 0.509$). Furthermore, the interaction between the two factors was not significant ($F_{(5,13)} = 0.08$, $P = 0.9958$). Paired t -tests between placebo and alcohol sessions only revealed a significant difference in theta rhythm ($P = 0.0095$). The Spearman's correlation analysis between EEG power and aDMN-DAN anti-correlation revealed no correlation in other frequency bands (delta: $P = 0.0673$, alpha 1: $P = 0.2799$, alpha 2: $P = 0.5536$, beta 1: $P = 0.0881$, and beta 2: $P = 0.8206$).

DISCUSSION

In this study we employed simultaneous EEG-fMRI to investigate the acute effects of alcohol on band-limited EEG power and their potential link with the functional interactions between DAN and DMN. Alcohol intoxication yielded an increased DMN-DAN anti-correlation, which was related to increased neuronal oscillations in the theta (4–8 Hz) band. Furthermore, increased theta power and increased DMN-DAN interactions were most prominent for participants who reported feeling intense euphoria,

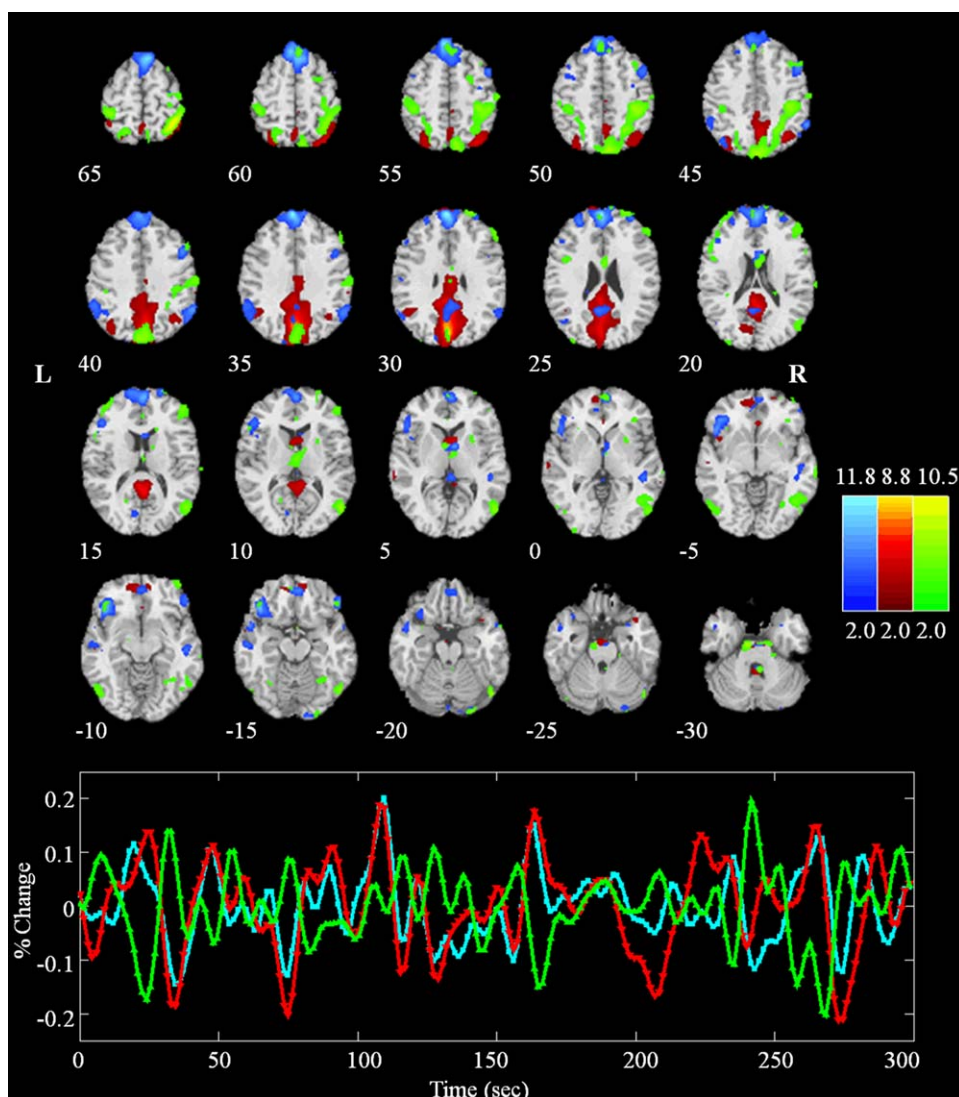


Figure 3.

Anterior (blue) and posterior (red) DMN and the DAN (green) in a single subject (placebo session). Brain areas with intensities of two standard deviations above the mean are shown in the spatial maps. The time courses of the networks were first regressed out global signal and then displayed with the same col-

ors of the corresponding maps. Note that the anterior part of DMN (aDMN) positively correlates with the posterior part of DMN (pDMN) and negatively correlates with the DAN. [Color figure can be viewed in the online issue, which is available at wileyonlinelibrary.com.]

suggesting inhibition exerted by the prefrontal cortex was diminished. On a more general level, our findings regarding alcohol-induced changes in neuronal (EEG) and hemodynamic (fMRI) measures support the idea that slow brain rhythms are primarily responsible for dynamic functional interactions between distinct brain networks [Ganzetti and Mantini, 2013].

Our EEG results revealed a relative power increase between alcohol and placebo conditions in the theta band (see Fig. 5), as already documented in early EEG investiga-

tions [Ehlers et al., 1989; Sanz-Martin et al., 2011; Schwarz et al., 1981; Tran et al., 2004]. More recent studies have related this specific EEG signature to an increased sensation of euphoria induced by alcohol. Specifically, Tran and colleagues interpreted this finding as a result of low cortical arousal during the ascending phase of alcohol intoxication [Tran et al., 2004], whereas Schwarz and coworkers suggested that the theta power increase is instead due to a de-inhibition [Schwarz et al., 1981]. A further issue left unresolved by EEG studies concerns the neuronal

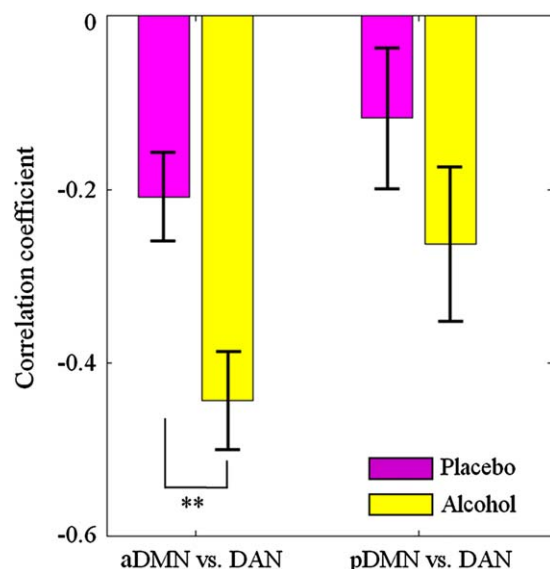


Figure 4.

Increased anti-correlation between DMN and DAN. The bar plots show the correlation coefficients (mean \pm standard error) between DAN and the anterior and posterior part of DMN in alcohol and placebo sessions. Significant changes between conditions were assessed by means of paired *t*-tests. Double asterisks indicate significant differences ($P < 0.01$). [Color figure can be viewed in the online issue, which is available at wileyonlinelibrary.com.]

generators of this specific theta-band activity. A magnetoencephalography study suggested that sources of theta rhythm are located along the frontal midline, in the prefrontal medial superficial cortex and anterior cingulate cortex (ACC) [Asada et al., 1999]. However, our EEG scalp topography data showed that theta power differences between alcohol and placebo were not confined to the frontal cortex, but extended to, and are more prominent over, the posterior parietal cortex (see the topography at 6 Hz in Fig. 5). This suggests that modulations in the power of brain rhythms induced by alcohol intoxication may reflect different neuronal processes, even in the same frequency band. For instance, it has also been proposed that the theta rhythm is a marker of fatigue [Craig et al., 2012]. Increased theta power is often accompanied by lower cognitive capacity and control, as reflected by slower reaction times and by attentional lapses [Klimesch, 1999; Makeig and Jung, 1996]. Neuroimaging studies are warranted to understand which brain systems are affected by alcohol intoxication, and in combination with EEG investigations can help to disentangle the neuronal mechanisms involved.

Previous fMRI studies identified global decreases in cortical activation after alcohol administration. However, activity levels in the DMN and DAN were found to be largely unaffected by alcohol administration [Esposito et al., 2010; Khalili-Mahani et al., 2012]. Note that our

fMRI analyses were not focused on activity levels in the DMN and DAN, but on the coupling between the time courses of these two networks. It should be mentioned that our study is not the first to examine changes in large-scale brain networks after alcohol administration. For instance, it was reported that inter-regional connectivity within frontal-temporal-basal ganglia and the cerebellum was impaired during simulated driving [Rzepecki-Smith et al., 2010]. Furthermore, another fMRI study on alcohol intoxication reported a dose-dependent increase in DAN activity and a dose-dependent decrease in activity in the precuneus/posterior cingulate, a core area of the DMN, during a visual perception task [Calhoun et al., 2004]. Based on the above findings and on the fact that the DMN and the DAN are respectively deactivated and activated during the performance of several cognitive tasks, we reasoned that the DMN-DAN anti-correlation should increase after alcohol administration. Our EEG-fMRI results (Fig. 6) confirmed this hypothesis, and provided us with a possible electrophysiological correlate of this DMN-DAN interaction.

Simultaneous EEG-fMRI has already been shown to be a valid tool with which to examine how changes in neuronal oscillations may be linked to functional interactions within and between brain networks [Mantini et al., 2007b; Lei et al., 2010, 2011b, 2012]. A large number of simultaneous EEG-fMRI studies revealed widespread negative correlations between band-limited EEG power and BOLD activity in the neocortex, but also produced positive correlations, as in the thalamus, for example [Goldman et al., 2002; Wu et al., 2010]. Specifically, the theta rhythm showed negative correlation with BOLD activity in the prefrontal cortex near the ACC [Martinez-Montes et al., 2004]. The negative correlations were extended to other areas that together form the default mode network [Scheeringa et al., 2008]. In our previous EEG-fMRI study in subjects at rest, we documented that multiple brain rhythms can account for activity within fMRI resting state networks [Mantini et al., 2007b]. During a condition of eyes-closed rest, for instance, alpha power showed a significant inverse relationship with the strength of connectivity between DMN and DAN [Chang et al., 2013].

Importantly, by using simultaneous EEG-fMRI we compared electrophysiological and hemodynamic measures of brain activity without confounds that are always present when the same participant is tested on the same experiment at two separate times [Debener et al., 2006]. It is indeed important to note that differences in participant's mood, vigilance, and behavior are likely to result in different patterns of brain activity. Furthermore, it would have been impossible to have in our study identical BAC levels in the same participant for separate EEG and fMRI acquisition sessions. The above factors would have made the EEG and fMRI data collected separately in the same participant not perfectly comparable.

In our study, we found two networks to be largely overlapping with the DMN, one more anterior (aDMN) and

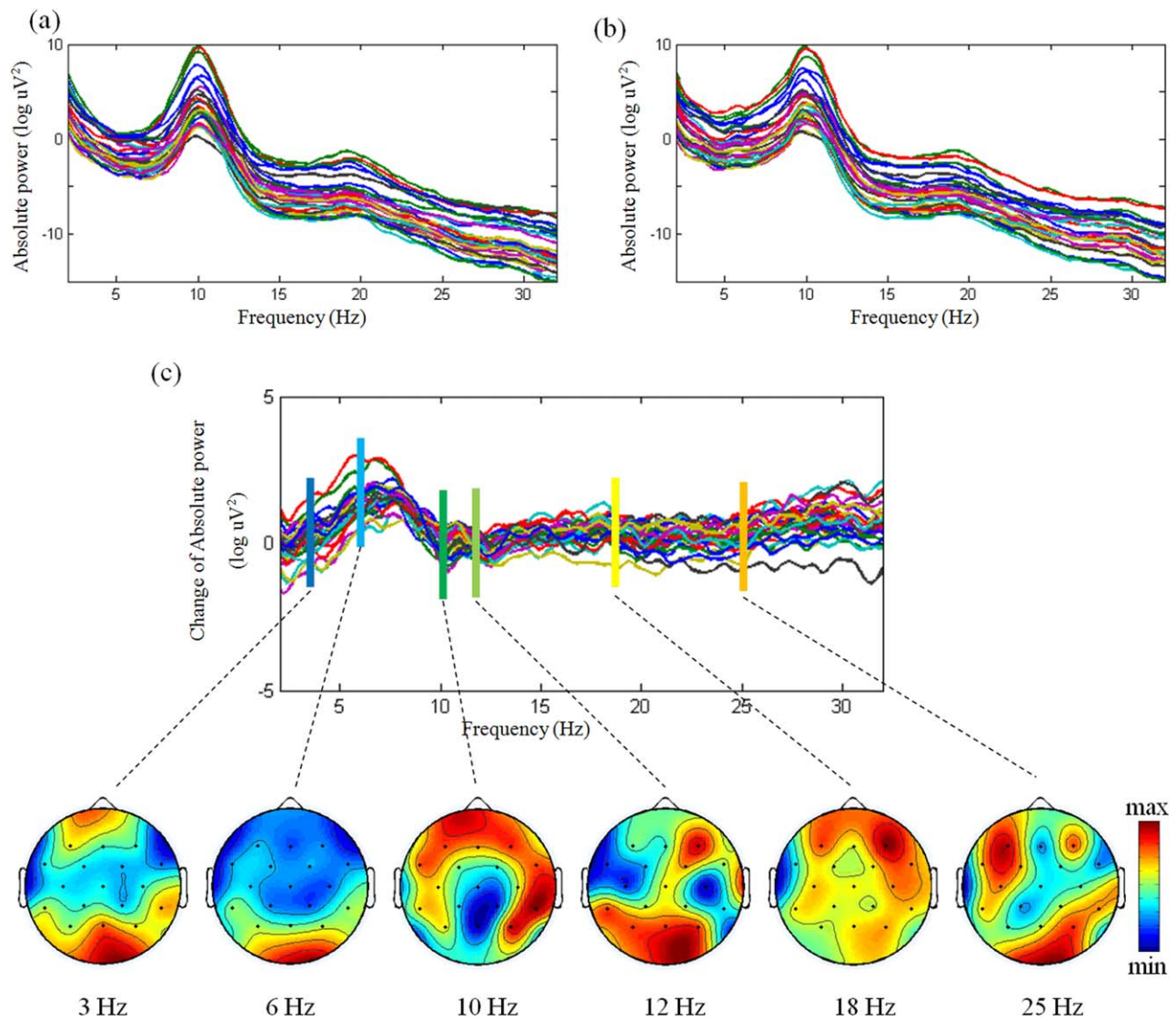


Figure 5.

Power spectra of all channels in (a) placebo and alcohol (b) sessions, and their difference (c). For the difference between alcohol and placebo, the topographies of EEG are illustrated in 3, 6, 10, 12, 18, 25 Hz. [Color figure can be viewed in the online issue, which is available at wileyonlinelibrary.com.]

one posterior (pDMN). Though many resting state studies have described a single DMN, a distinction between aDMN and pDMN has been previously reported [Damoiseaux et al., 2008; Lei et al., 2013]. Interestingly, we found aDMN to be more strongly anti-correlated with the DAN compared to pDMN. Furthermore, the strength of the interaction between aDMN and DAN was correlated with the power of the theta rhythm but not that of other rhythms, and was more prominent over prefrontal areas (Fig. 4). Insofar as both our EEG and fMRI findings converge on medial frontal areas, it is tantalizing to link them

to the reported effects of alcohol on the reward system, particularly the ACC. Alcoholism has often been linked with decreased grey matter volume [Makris et al., 2008] and decreased neural activity in the reward circuit [De Greck et al., 2009; Wrase et al., 2007]. Decreased activations in ACC and cerebellum were found during a working memory task after moderate alcohol intoxication [Gundersen et al., 2008]. Also, acute alcohol intoxication impaired behavioral performance and selectively attenuated ACC activation during conflict-inducing tasks [Marinkovic et al., 2011]. In our study, the lack of DMN

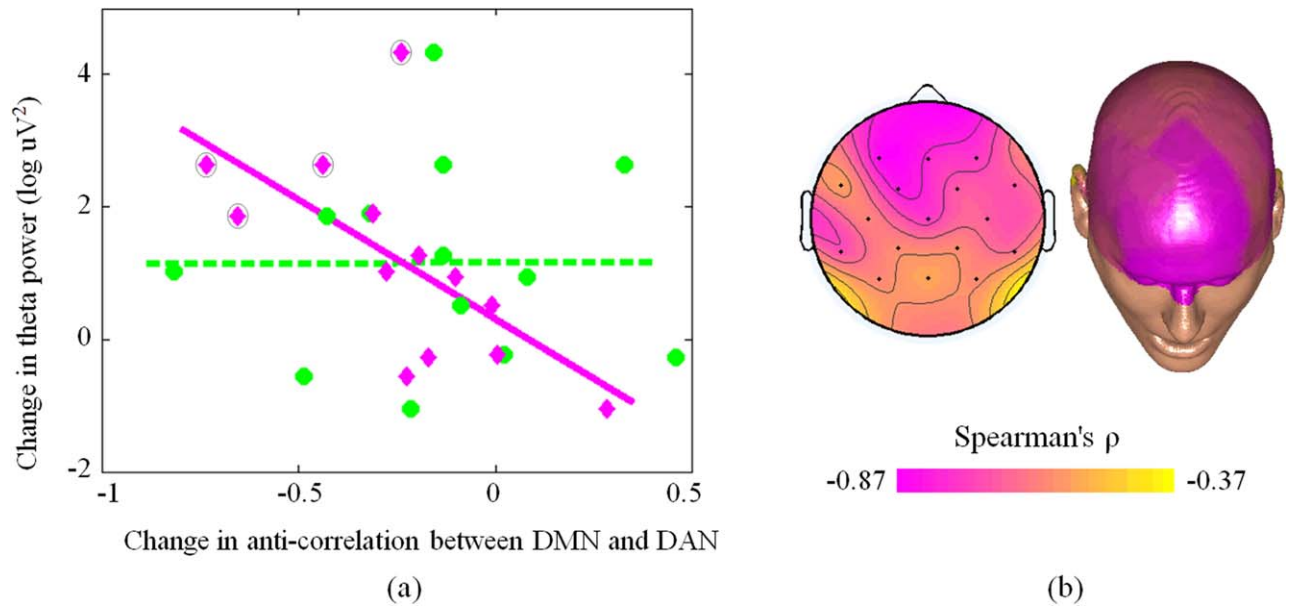


Figure 6.

Relationship between changes in DMN-DAN anti-correlation and theta power EEG activity across subjects. (a) The pink line indicates the correlation between change in anti-correlation between DAN and aDMN, whereas each pink diamond represents a single subject. The green dotted line indicates the correlation between change in anti-correlation between DAN and pDMN, whereas each green circle represents a given subject. A

pink diamond outlined in a black circle represents an individual reporting intense euphoria. (b) The correlation between theta rhythm power in each EEG channel and anti-correlation between DAN and DMN is represented in a topographical EEG map. [Color figure can be viewed in the online issue, which is available at wileyonlinelibrary.com.]

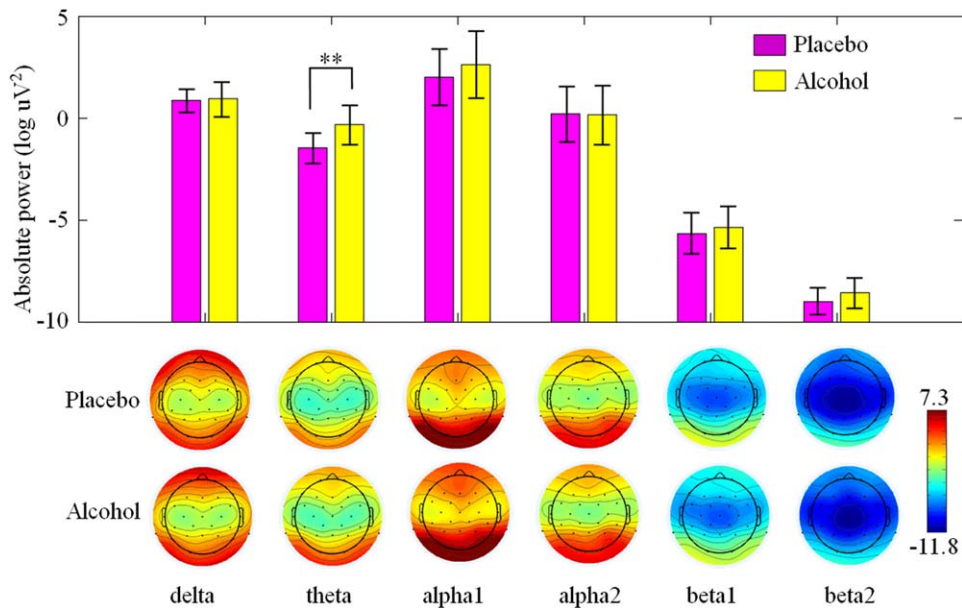


Figure 7.

The grand-average absolute powers (mean \pm standard error) and topographies of EEG bands (delta, theta, alpha 1, alpha 2, beta 1, and beta 2) in placebo and alcohol sessions. [Color figure can be viewed in the online issue, which is available at wileyonlinelibrary.com.]

suppression, mainly in medial frontal areas, may be related to the excitatory (or dis-inhibitory) effects of alcohol. Many behavioral studies have shown euphoric sensations after alcohol consumption to be a correlate of diminished self-inhibition [Levin et al., 1998; Schwarz et al., 1981]. Accordingly, our results lend support to the idea that reduced inhibitory control induced by alcohol intoxication is reflected by a larger functional interaction between DMN and DAN, possibly implemented at the neuronal level by oscillations in the theta band.

Our simultaneous EEG-fMRI study of alcohol intoxication has permitted us to obtain valuable information regarding the possible link between neuronal oscillations and functional interaction between brain networks. However, it is important to mention that our study has a number of limitations. Firstly, EEG data collected during fMRI scanning are contaminated by strong artifacts. We have attenuated artifacts in the data, but this procedure may have also suppressed some brain activity. Secondly, we used a 32-channels EEG system, which does not permit accurate source localizations. For this reason, we analyzed EEG recordings using grand averages over channels, and we did not examine EEG activity in the source space [Lei et al., 2011b]. Thirdly, applying ICA to fMRI data captures only a part of brain activity, and because we also focused on DAN and DMN, the effects of alcohol on other networks should be examined in future studies [Lei et al., 2011a]. Finally, although our results linking EEG theta and the DMN-DAN interaction are quite specific, our findings need to be replicated in a larger group of subjects.

In conclusion, we used simultaneous EEG-fMRI to investigate the relationship between changes in neuronal oscillations and functional interactions between resting state networks, following alcohol intoxication. Specifically, we found that heightened DMN-DAN anti-correlation was related to an increase in the power of the theta rhythm. Importantly, our findings support the concept that slow brain rhythms are responsible for dynamic functional interactions between distinct brain networks. They also confirm the applicability and potential usefulness of resting-state EEG-fMRI for central nervous system drug research.

REFERENCES

- Allen PJ, Josephs O, Turner R (2000): A method for removing imaging artifact from continuous EEG recorded during functional MRI. *Neuroimage* 12:230–239.
- Asada H, Fukuda Y, Tsunoda S, Yamaguchi M, Tonoike M (1999): Frontal midline theta rhythms reflect alternative activation of prefrontal cortex and anterior cingulate cortex in humans. *Neurosci Lett* 274:29–32.
- Bressler SL, Menon V (2010): Large-scale brain networks in cognition: Emerging methods and principles. *Trends Cogn Sci* 14: 277–290.
- Buckner RL, Andrews-Hanna JR, Schacter DL (2008): The brain's default network: Anatomy, function, and relevance to disease. *Ann NY Acad Sci* 1124:1–38.
- Calhoun VD, Adali T, Pearlson GD, Pekar JJ (2001a): A method for making group inferences from functional MRI data using independent component analysis. *Hum Brain Mapp* 14:140–151.
- Calhoun VD, Adali T, Pearlson GD, Pekar JJ (2001b): Spatial and temporal independent component analysis of functional MRI data containing a pair of task-related waveforms. *Hum Brain Mapp* 13:43–53.
- Calhoun VD, Altschul D, McGinty V, Shih R, Scott D, Sears E, Pearlson GD (2004): Alcohol intoxication effects on visual perception: An fMRI study. *Hum Brain Mapp* 21:15–25.
- Chang C, Liu Z, Chen MC, Liu X, Duyn JH (2013): EEG correlates of time-varying BOLD functional connectivity. *Neuroimage* 72: 227–236.
- Corbetta M, Shulman GL (2002): Control of goal-directed and stimulus-driven attention in the brain. *Nat Rev Neurosci* 3: 201–215.
- Craig A, Tran Y, Wijesuriya N, Nguyen H (2012): Regional brain wave activity changes associated with fatigue. *Psychophysiology* 49:574–582.
- Damoiseaux JS, Beckmann CF, Arigita EJ, Barkhof F, Scheltens P, Stam CJ, Smith SM, Rombouts SA (2008): Reduced resting-state brain activity in the "default network" in normal aging. *Cereb Cortex* 18:1856–1864.
- de Greck M, Supady A, Thiemann R, Tempelmann C, Bogerts B, Forschner L, Ploetz KV, Northoff G (2009): Decreased neural activity in reward circuitry during personal reference in abstinent alcoholics—A fMRI study. *Hum Brain Mapp* 30:1691–1704.
- De Pisapia N, Turatto M, Lin P, Jovicich J, Caramazza A (2012): Unconscious priming instructions modulate activity in default and executive networks of the human brain. *Cereb Cortex* 22: 639–649.
- Debener S, Ullsperger M, Siegel M, Engel AK (2006): Single-trial EEG-fMRI reveals the dynamics of cognitive function. *Trends Cogn Sci* 10:558–563.
- Ehlers CL, Wall TL, Schuckit MA (1989): EEG spectral characteristics following ethanol administration in young men. *Electroencephalogr Clin Neurophysiol* 73:179–187.
- Esposito F, Pignataro G, Di Renzo G, Spinale A, Paccone A, Tedeschi G, Annunziato L (2010): Alcohol increases spontaneous BOLD signal fluctuations in the visual network. *Neuroimage* 53:534–543.
- Fornito A, Harrison BJ, Zalesky A, Simons JS (2012): Competitive and cooperative dynamics of large-scale brain functional networks supporting recollection. *Proc Natl Acad Sci USA* 109: 12788–12793.
- Fox MD, Snyder AZ, Vincent JL, Corbetta M, Van Essen DC, Raichle ME (2005): The human brain is intrinsically organized into dynamic, anticorrelated functional networks. *Proc Natl Acad Sci USA* 102:9673–9678.
- Fox MD, Zhang D, Snyder AZ, Raichle ME (2009): The global signal and observed anticorrelated resting state brain networks. *J Neurophysiol* 101:3270–3283.
- Fransson P (2006): How default is the default mode of brain function? Further evidence from intrinsic BOLD signal fluctuations. *Neuropsychologia* 44:2836–2845.
- Ganzetti M, Mantini D (2013): Functional connectivity and oscillatory neuronal activity in the resting human brain. *Neuroscience* 240:297–309.

- Goldman RI, Stern JM, Engel J Jr, Cohen MS (2002): Simultaneous EEG and fMRI of the alpha rhythm. *Neuroreport* 13:2487–2492.
- Gundersen H, Specht K, Gruner R, Erslund L, Hugdahl K (2008): Separating the effects of alcohol and expectancy on brain activation: An fMRI working memory study. *Neuroimage* 42:1587–1596.
- Kelly AMC, Uddin LQ, Biswal BB, Castellanos FX, Milham MP (2008): Competition between functional brain networks mediates behavioral variability. *Neuroimage* 39:527–537.
- Khalili-Mahani N, Zoethout RM, Beckmann CF, Baerends E, de Kam ML, Soeter RP, Dahan A, van Buchem MA, van Gerven JM, Rombouts SAR (2012): Effects of morphine and alcohol on functional brain connectivity during “resting state”: A placebo-controlled crossover study in healthy young men. *Hum Brain Mapp* 33:1003–1018.
- Klimesch W (1999): EEG alpha and theta oscillations reflect cognitive and memory performance: A review and analysis. *Brain Res Brain Res Rev* 29:169–195.
- Laufs H, Krakow K, Sterzer P, Eger E, Beyerle A, Salek-Haddadi A, Kleinschmidt A (2003): Electroencephalographic signatures of attentional and cognitive default modes in spontaneous brain activity fluctuations at rest. *Proc Natl Acad Sci USA* 100:11053–11058.
- Lee MH, Hacker CD, Snyder AZ, Corbetta M, Zhang D, Leuthardt EC, Shimony JS (2012): Clustering of resting state networks. *Plos One* 7:e40370.
- Lei X, Ostwald D, Hu J, Qiu C, Porcaro C, Bagshaw AP, Yao D (2011a): Multimodal functional network connectivity: An EEG-fMRI fusion in network space. *Plos One* 6:e24642.
- Lei X, Qiu C, Xu P, Yao D (2010): A parallel framework for simultaneous EEG/fMRI analysis: Methodology and simulation. *Neuroimage* 52:1123–1134.
- Lei X, Valdes Sosa P, Yao D (2012): EEG/fMRI fusion based on independent component analysis: Integration of data-driven and model-driven methods. *J Integr Neurosci* 11:1–25.
- Lei X, Xu P, Luo C, Zhao J, Zhou D, Yao D (2011b): fMRI Functional Networks for EEG Source Imaging. *Human Brain Mapping* 32:1141–1160.
- Lei X, Zhao Z, Chen H (2013): Extraversion is encoded by scale-free dynamics of default mode network. *Neuroimage* 74:52–57.
- Levin JM, Ross MH, Mendelson JH, Kaufman MJ, Lange N, Maas LC, Mello NK, Cohen BM, Renshaw PF (1998): Reduction in BOLD fMRI response to primary visual stimulation following alcohol ingestion. *Psychiatry Res* 82:135–146.
- Li YO, Adali T, Calhoun VD (2007): Estimating the number of independent components for functional magnetic resonance imaging data. *Hum Brain Mapp* 28:1251–1266.
- Lukas SE, Mendelson JH, Benedikt RA, Jones B (1986): EEG alpha activity increases during transient episodes of ethanol-induced euphoria. *Pharmacol Biochem Behav* 25:889–895.
- Makeig S, Jung TP (1996): Tonic, phasic, and transient EEG correlates of auditory awareness in drowsiness. *Brain Res Cogn Brain Res* 4:15–25.
- Makris N, Oscar-Berman M, Jaffin SK, Hodge SM, Kennedy DN, Caviness VS, Marinkovic K, Breiter HC, Gasic GP, Harris GJ (2008): Decreased volume of the brain reward system in alcoholism. *Biol Psychiatry* 64:192–202.
- Mantini D, Caulo M, Ferretti A, Romani G, Tartaro A (2009): Noxious somatosensory stimulation affects the default mode of brain function: Evidence from functional MR imaging. *Radiology* 253:797–804.
- Mantini D, Corbetta M, Romani GL, Orban GA, Vanduffel W (2013): Evolutionarily novel functional networks in the human brain? *J Neurosci* 33:3259–3275.
- Mantini D, Perrucci MG, Cugini S, Ferretti A, Romani GL, Del Gratta C (2007a): Complete artifact removal for EEG recorded during continuous fMRI using independent component analysis. *Neuroimage* 34:598–607.
- Mantini D, Perrucci MG, Del Gratta C, Romani GL, Corbetta M (2007b): Electrophysiological signatures of resting state networks in the human brain. *Proc Natl Acad Sci USA* 104:13170–13175.
- Mantini D, Vanduffel W (2013): Emerging roles of the brain’s default network. *Neuroscientist* 19:76–87.
- Marinkovic K, Rickenbacher E, Azma S, Artsy E (2011): Acute alcohol intoxication impairs top-down regulation of stroop incongruity as revealed by blood oxygen level-dependent functional magnetic resonance imaging. *Hum Brain Mapp* 33:319–333.
- Martinez-Montes E, Valdes-Sosa PA, Miwakeichi F, Goldman RI, Cohen MS (2004): Concurrent EEG/fMRI analysis by multiway Partial Least Squares. *Neuroimage* 22:1023–1034.
- Niazy RK, Beckmann CF, Iannetti GD, Brady JM, Smith SM (2005): Removal of fMRI environment artifacts from EEG data using optimal basis sets. *Neuroimage* 28:720–737.
- Rzepecki-Smith CL, Meda SA, Calhoun VD, Stevens MC, Jafri MJ, Astur RS, Pearlson GD (2010): Disruptions in functional network connectivity during alcohol intoxicated driving. *Alcohol Clin Exp Res* 34:479–487.
- Sanz-Martin A, Guevara MÁ, Amezcua C, Santana G, Hernández-González M (2011): Effects of red wine on the electrical activity and functional coupling between prefrontal-parietal cortices in young men. *Appetite* 57:84–93.
- Scheeringa R, Bastiaansen MC, Petersson KM, Oostenveld R, Norris DG, Hagoort P (2008): Frontal theta EEG activity correlates negatively with the default mode network in resting state. *Int J Psychophysiol* 67:242–251.
- Schwarz E, Kielholz P, Hobi V, Goldberg L, Gilsdorf U, Hofstetter M, Ladewig D, Miest PC, Reggiani G, Richter R (1981): Alcohol-induced biphasic background and stimulus-elicited EEG changes in relation to blood alcohol levels. *Int J Clin Pharmacol Ther Toxicol* 19:102–111.
- Tran Y, Craig A, Bartrop R, Nicholson G (2004): Time course and regional distribution of cortical changes during acute alcohol ingestion. *Int J Neurosci* 114:863–878.
- Van Dijk KRA, Hedden T, Venkataraman A, Evans KC, Lazar SW, Buckner RL (2010): Intrinsic functional connectivity as a tool for human connectomics: Theory, properties, and optimization. *J Neurophysiol* 103:297–321.
- Wrase J, Schlagenhauf F, Kienast T, Wustenberg T, Berman F, Kahnt T, Beck A, Strohle A, Juckel G, Knutson B, Heinz A (2007): Dysfunction of reward processing correlates with alcohol craving in detoxified alcoholics. *Neuroimage* 35:787–794.
- Wu L, Eichele T, Calhoun VD (2010): Reactivity of hemodynamic responses and functional connectivity to different states of alpha synchrony: A concurrent EEG-fMRI study. *Neuroimage* 52:1252–1260.
- Zuo XN, Kelly C, Adelstein JS, Klein DF, Castellanos FX, Milham MP (2010): Reliable intrinsic connectivity networks: Test-retest evaluation using ICA and dual regression approach. *Neuroimage* 49:2163–2177.